Polyhedron 56 (2013) 211–220

Contents lists available at SciVerse ScienceDirect

Polyhedron

journal homepage: www.elsevier.com/locate/poly

A palladium(II) complex: Synthesis, structure, characterization, electrochemical behavior, thermal aspects, BVS calculation and antimicrobial activity

Chiranjan Biswas [a], Miaoli Zhu [b], Liping Lu [b], Sudipta Kaity [c], Mousumi Das [c], Amalesh Samanta [c], Jnan Prakash Naskar [a,*]

[a] Department of Chemistry, Jadavpur University, Calcutta 700 032, India
[b] Institute of Molecular Science, Key Laboratory of Chemical Biology and Molecular Engineering of the Education Ministry, Shanxi University, 92 Wucheng Road, Taiyuan, Shanxi 030006, People's Republic of China
[c] Division of Microbiology, Department of Pharmaceutical Technology, Jadavpur University, Calcutta 700 032, India

ARTICLE INFO

Article history:
Received 9 January 2013
Accepted 26 March 2013
Available online 10 April 2013

Keywords:
Oxime
Palladium
Structure
BVS
Redox
Cytotoxicity

ABSTRACT

The reaction of equimolar proportions of $Na_2[PdCl_4]$ and 1-(4-methylimidazol-5-yl) phenylhydrazonopropane-2-one oxime (LH), a 1:1 Schiff-base condensate of 1-hydrazono-1-phenyl-propan-2-one oxime (**1**) and 4-methylimidazole-5-carboxaldehyde, in methanol gives rise to [Pd(L)(Cl)] (**2**) in a satisfactory yield. The title monomeric palladium(II) complex, **2**, has been characterized by C, H and N microanalyses, ^1H and ^{13}C NMR, FAB-MS, FT-IR, UV–Vis spectra, molar electric conductivity measurements and room temperature magnetic susceptibility measurements. The X-ray crystal structures of **1** and **2** have been determined. The structure of **1**, a precursor of the ligand (LH), shows that the methyl and phenyl groups are in an '*anti*' disposition. Compound **1** crystallizes in the monoclinic space group $P2_1$ with $a = 6.9503(5)$, $b = 6.4535(3)$, $c = 10.1631(6)$ Å, $V = 455.04(5)$ Å^3 and $Z = 2$. The structure of **2** reveals that it is a distorted square-planar palladium(II) compound. The palladium center is in an 'N_3Cl' coordination chromophore. Complex **2** crystallizes in the tetragonal space group $I4_1/a$ with $a = 22.5744(3)$, $b = 22.5744(3)$, $c = 13.2967(2)$ Å, $V = 6776.05(16)$ Å^3 and $Z = 16$. The thermal and electrochemical aspects of **2** have been studied. Electrochemical studies in DMF show a Pd(II) to Pd(III) oxidation at 0.573 V, along with a reduction of Pd(II) to Pd(I) at −0.757 V versus Ag/AgCl. A Bond-Valence Sum (BVS) model calculation was performed to assign the oxidation state of the palladium center in **2**. The *in vitro* antimicrobial activity of **2** was tested against both Gram positive and Gram negative bacteria. Complex **2** exhibits satisfactory bacteriostatic activity.

1. Introduction

In terms of annual demand, palladium is one of the most important platinum group metals [1]. Pd(II) complexes have attracted renewed interest due to their wide-spread applications in organic syntheses [2], catalytic processes [3], biological and pharmacological usage [4]. The palladium catalyzed Suzuki–Miyaura cross-coupling reaction represents one of the most widely used processes for the synthesis of biaryls [5–8]. In addition, palladium-catalyzed Heck reactions of aryl halides with alkenes have also become one of the most powerful tools in organic synthesis for the making of the carbon–carbon bond [9,10]. The use of Pd-catalysts in Suzuki–Miyaura and Heck-Mizoroki cross-coupling reactions in aqueous media stems interest from a viewpoint of green sustainable chemistry [11,12]. Apart from catalytic aspects, Pd(II) compounds have inherent cytotoxic behavior. On the basis of the structural analogy (d^8 ions in a square-planar geometry) and the thermodynamic difference with Pt(II) complexes, there is much interest in the study of palladium(II) complexes as potential anticancer drugs, especially those bearing the chelating ligands [13–15]. In this context it is interesting to note that the first monomeric Pd(II) complex having excellent antiproliferative activity, as demonstrated by *in vitro* experiments, was a mixed ligand Pd(II) complex [16]. The associated ligand was, as usual, a thiosemicarbazone based ligand with triphenyl phosphine as an ancillary ligand [17,18]. Curiously such type of bioactivity of a monomeric Pd(II) compound with an N,O-donor oxime-based ligand is unprecedented. Herein we wish to report the synthesis, characterization, structure, thermal and redox behavior of a monomeric Pd(II) complex synthesized from an oxime-based ligand. The antimicrobial activity of the ligand, 1-(4-methylimidazol-5-yl) phenylhydrazonopropane-2-one oxime (LH), and its palladium(II) compound, **2** was investigated against

* Corresponding author. Fax: +91 33 2414 6223.
E-mail addresses: asamanta61@yahoo.co.in (A. Samanta), jpnaskar@rediffmail.com (J.P. Naskar).

0277-5387/$ - see front matter © 2013 Elsevier Ltd. All rights reserved.
http://dx.doi.org/10.1016/j.poly.2013.03.064

seventeen bacterial cell lines. Semi-empirical BVS calculations were also undertaken to assign the oxidation state of the central palladium ion.

2. Experimental

2.1. Materials and measurements

All chemicals were of analytical reagent grade and used without further purification. Palladium chloride and 4-methylimidazole-5-carboxaldehyde were purchased from Sigma–Aldrich Chemicals Pvt. Ltd. 1-Hydrazono-1-phenyl-propan-2-one oxime was prepared by a procedure reported herein. The melting point was determined by an electro-thermal digital melting point apparatus (SUMSIM India) and is uncorrected. Microanalyses were performed with a Perkin-Elmer 2400II elemental analyser. FTIR spectra (KBr disc) [(vs) = very strong, (s) = strong, (m) = medium and (w) = weak] were recorded with a Nicolet Magna-IR spectrophotometer (Series II). UV–Vis spectra (in DMF) were recorded on a Shimadzu UV-160A spectrophotometer. 300 MHz ^{1}H NMR spectra of the ligand precursor, **1** and LH (in $CDCl_3$: reference, TMS) were recorded on a Bruker DPX300 spectrometer and the ^{13}C NMR spectrum (observed frequency: 126 MHz) of LH (in DMSO-d_6 with reference to TMS) on a Bruker DPX500 spectrometer. 500 MHz ^{1}H and ^{13}C NMR spectra (observed frequency: 126 MHz for ^{13}C) of the Pd(II) compound **2** were recorded in DMSO-d_6 with reference to TMS on a Bruker DPX500 spectrometer. The FAB mass spectra in the positive ionization mode were recorded in *m*-nitrobenzyl alcohol (MNBA) matrix on a JEOL Mass spectrometer (Model: JMS-700), Japan. Solution conductivity measurements of **2** were carried out in DMF and DMSO at room temperature on a Systronics (India) direct reading conductivity meter (Model 304). Cyclic voltammetric (CV) experiments were performed under nitrogen in dry and degassed DMF using a BAS Epsilon electrochemical workstation at 298 K. The conventional three-electrode assembly is comprised of a Glassy Carbon (GC) working electrode, a platinum-wire auxiliary electrode and an Ag/AgCl reference electrode. The supporting electrolyte is *n*-Bu_4NClO_4 (0.1 M). Thermal analyses (TGA/DTA) were performed under a dynamic nitrogen atmosphere (20.00 mL/min) on a Perkin-Elmer instrument (Model: Pyris Diamond TG/DTA). Magnetic susceptibility was determined at room temperature with a PAR 155 vibrating sample magnetometer fitted with a walker scientific L75FBAL magnet. The magnetometer was calibrated with $Hg[Co(SCN)_4]$.

The microorganisms used in the present antimicrobial study consisted of 17 bacterial strains, namely *Escherichia coli* ATCC 25938, *Salmonella typhi* 62, *Pseudomonas* AMRI 100, *Vibrio cholerae* VC 20, *Klebsiella pneumoniae* 714, *Shigella dysenteriae* 1, *Staphyloccus aureus* 29737, *Bacillus cereus* 11778, *Pseudomonas aeruginosa* 25619, *Bacillus subtilis* 6633, *Bacillus pumilus* 14884, *Bacillus bronchiseptica* 4617, *Streptococcus epidermidis* 12228, *Klebsiella pneumoniae* 10031, *Micrococcus luteus* 10240, *Shigella sonnei* NK 4010 and *Salmonella typhimurium* NTCC 74. The bacterial strains were obtained from the Division of Microbiology, Department of Pharmaceutical Technology, Jadavpur University, Kolkata, India.

2.1.1. Preparation of the ligand

*2.1.1.1. Preparation of 1-hydrazono-1-phenyl-propan-2-one oxime (**1**).* 1.0 g (6.132 mmol) of 1-phenyl-1,2- propanedione-2-oxime was dissolved in 5 mL of dry methanol to give a colorless solution. Then 0.3 mL (6.132 mmol) of hydrazine hydrate was added dropwise with constant stirring to the oxime solution. Gradually the solution became light yellow and the resulting solution was stirred for 3 h. At the end of stirring, it was left in air for slow evaporation. After 24 h, shining light yellow needle shaped crystalline compounds separated. These were filtered, washed with 5 mL of chilled methanol and subsequently dried in a vacuum desiccator over fused $CaCl_2$. The product (**1**) is partly soluble in chloroform, acetone and also in methanol. Yield: 872 mg (80%). M.p.: 162–164 °C. $C_9H_{11}N_3O$ (177.088): *Anal.* Calc. for $C_9H_{11}N_3O$: C, 60.99; H, 6.26; N, 23.72. Found: C, 60.84; H, 6.27; N, 23.82%. FTIR (KBr) ν [cm^{-1}]: 3389(s) [ν(OH)], 3283(s) [$\nu(NH_2)$], 1569(s) [ν(C=N) of imine], 1467(s) [ν(C=N) of oxime], 1208(s) [ν(N–O)]. ^{1}H NMR (300 MHz, $CDCl_3$, TMS) δ [ppm]: 7.86 (2H, d, ortho-hydrogens of the phenyl group attached to C2 and C6), 7.47 (2H, t, meta-hydrogens of phenyl ring attached to C3 and C5), 7.42 (1H, t, para-hydrogen of phenyl ring attached to C4), 7.18 (2H, s, hydrogens of the free amine group), 2.15 (3H, s, methyl proton attached to C9), UV–Vis (DMF) λ_{max}[nm] (ε_{max}[M^{-1} cm^{-1}]): 273 (1.1504×10^4).

Crystals suitable for X-ray structure determination were obtained by slow aerial evaporation of a moderately concentrated solution of **1** in methanol.

2.1.1.2. 1-(4-Methylimidazol-5-yl) phenylhydrazonopropane-2-one oxime, LH. 100 mg (0.565 mmol) of 1-hydrazono-1-phenyl-propan-2-one oxime (**1**) was dissolved in 15 mL of hot methanol to get a light yellow solution. To this solution was added 62 mg (0.564 mmol) of solid 4-methylimidazole-5-carboxaldehyde, which was thoroughly dissolved. The reaction mixture was heated under reflux for 4 h. Within 15 min of refluxing, a yellow color was obtained. After refluxing, the dark yellow reaction mixture was left in air for slow evaporation. After 2 days, the precipitated yellow compound that was obtained was filtered, washed thoroughly with diethyl ether and then dried in a vacuum desiccator over fused $CaCl_2$. The product, LH, is soluble in DMSO, chloroform and methanol upon heating, but insoluble in acetonitrile and dichloromethane even on heating. Yield: 100 mg (66%). M.p.: 192–194 °C. $C_{14}H_{15}N_5O$ (269.12): *Anal.* Calc. for $C_{14}H_{15}N_5O$: C, 62.43; H, 5.62; N, 26.01; Found: C, 62.54; H, 5.49; N, 26.31%. FTIR (KBr) ν [cm^{-1}]: 3293(vb) [ν(OH)], 1616(s) [ν(C=N)], 1462(s) [ν(C=N of oxime)], 1188(s) [ν(N–O)]. ^{1}H NMR (300 MHz, $CDCl_3$, TMS) δ [ppm]: >12 (methyl protons of imidazole ring attached to C14), 9.82 (oximato proton), 8.47(methylene proton adjacent to the imine attached to C10), 7.90 (ortho-hydrogens of the phenyl ring attached to C2 and C6), 7.61 (NH proton of the imidazole ring), 7.53 (CH proton of the imidazole ring attached to C12), 7.46 (meta-hydrogens of the phenyl ring attached to C3 and C5), 7.43 (para-hydrogen of the phenyl ring attached to C4), 2.19 (methyl protons attached to C9). ^{13}C NMR (126 MHz, DMSO-d_6, TMS) δ [ppm]: 162.9(C10), 155.7(C8), 154.9(C7), 135.3(C12), 134.1(C13), 129.2(C1), 128.6(C4), 127.5(C2,C6), 127.3(C3,C5), 127.0(C11), 11.1(C9), 10.0(C14). UV–Vis (MeOH) λ_{max}[nm] (ε_{max}[M^{-1} cm^{-1}]) = 320 (2.269×10^4), 233 (1.201×10^4), 203(1.996×10^4).

2.1.2. Preparation of [Pd(L)(Cl)] (**2**)

20 mg (0.074 mmol) of LH was dissolved in 10 mL of methanol to get a yellowish solution, then 21.88 mg (0.074 mmol) of $Na_2[PdCl_4]$ dissolved in 5 mL of methanol was added into the ligand solution dropwise with stirring at room temperature. The color of the solution gradually changed to dark brown. The resulting reaction mixture was left in air for slow evaporation. After 24 h shining rod shaped brown crystals which deposited were filtered, washed thoroughly with diethyl ether and dried in a vacuum desiccator over fused $CaCl_2$. Some of the brown crystals were fit for X-ray structure determination. Yield: 13 mg (43%). M. p.: >220 °C. $C_{14}H_{14}ClN_5OPd$ (410.15): *Anal.* Calc. for $C_{14}H_{14}ClN_5OPd$: C, 40.97; H, 3.44; N, 17.07. Found: C, 40.76; H, 3.21; N, 17.25%. FT-IR (KBr) ν [cm^{-1}]: 3038 (br) [ν(NH)], 1609(vs) [ν(C=N) of imine], 1451(m) [ν(C=N) of oxime], 1206(s) [ν(N–O)], 441(s) [ν(Pd–N)]. ^{1}H NMR (500 MHz, DMSO-d_6, TMS) δ [ppm]: 8.24 (1H, s, hydrogen of imine carbon attached to C10), 7.69 (1H, s, imidazole ring proton attached to C12), 7.48 (3H,

d, meta and para hydrogens of phenyl group attached to C3, C5 and C4), 7.35 (2H, d, ortho-hydrogens of the phenyl group attached to C2 and C6), 2.33 (3H, s, imidazole ring methyl protons attached to C14) 1.47 (3H, s, methyl protons attached to C9). ^{13}C NMR (126 MHz, DMSO-d_6, TMS) δ [ppm]: 176.8(C10), 147.7(C8), 141.6(C7), 138.2(C12), 137.5(C13), 133.3(C1), 130.0(C4), 128.9(C2,C6), 128.7(C3,C5), 118.9(C11), 12.5(C9), 9.3(C14). UV–Vis (DMF) λ_{max}[-nm] (ε_{max}[M^{-1} cm^{-1}]): 315 (1.012×10^4), 319 (1.014×10^4), 502 (3.452×10^3). FAB-MS (positive ion mode in *m*-nitrobenzyl alcohol matrix) (*m*/*z*): 374.1 for $[Pd(L)]^+$ (100%). Λ_M (DMF): 58 $\Omega^{-1}cm^2mol^{-1}$ (Non-conducting). Λ^M (DMSO): 11 Ω^{-1} cm^2 mol^{-1} (Non-conducting). μ = Diamagnetic.

2.2. Crystal structure determinations

Shining rod shaped brown single crystals of **2** suitable for X-ray crystallography were grown from the reaction mixture. Single crystals suitable for X-ray crystallographic analysis were selected following examination under a microscope. Intensity data were collected at 298(2) K for **1** and **2** on a Bruker Smart Apex II diffractometer equipped with a 1 K CCD instrument using a graphite monochromator with Mo Kα radiation (λ = 0.71073 Å). Cell parameters were determined using SMART software [19]. Data reduction and corrections were performed using SAINTPLUS [19]. Absorption corrections were made via SADBAS [20]. The structures were solved by direct methods with the program SHELXS-97 and refined by full-matrix least-squares methods on all F^2 data with SHELXL-97 [20]. The non-H atoms were refined anisotropically. Hydrogen atoms attached to C, N and O atoms were added theoretically and treated as riding on the concerned atoms. The final cycle of full-matrix least-squares refinement was based on observed reflections and variable parameters. Large void spaces for **2** accounting in total for 1745.2 Å^3 per unit cell, i.e. some 31.2% of the total volume, were examined using PLATON [21]. The reflection data were subjected to the SQUEEZE routine in PLATON before the final refinement and this suggested the presence of 156 electrons per unit cell within the voids, but we failed to define some solvent molecules. A summary of the data collection and structure refinement for **1** and **2** is given in Table 1. Selected bond lengths, bond angles and hydrogen-bond geometries are given in Tables 2 and 3 respectively.

2.3. Studies of antimicrobial activity

The antimicrobial activity of the ligand LH as well as the Pd(II) compound **2** were examined by *in vitro* testing. Seventeen microorganisms, both Gram positive and Gram negative, were used for this screening. Amoxycillin, a versatile antibacterial clinical therapeutic agent, was used as the reference material [22]. Compound **2** was primarily tested for screening by agar dilution [23], then susceptible organisms were selected and the Minimum Inhibitory Concentrations (MIC) were determined as per the NCCLS protocol [24] and by an INT assay (*p*-iodo-nitro-teterazolium chloride). Finally, considering the best result against a particular organism, the effect of **2** on bacterial growth rate was studied.

2.3.1. Preparation of inoculums

These strains were grown in Mueller-Hilton Agar (Merck India Ltd.) at 37 °C for 24 h and the suspension was prepared by matching a 0.5 McFarland standard [25].

2.3.2. Drug solution

A drug solution of the synthetic drug was prepared by dissolving analytically pure crystals of **2** in 1% DMSO solution along with sterile distilled water and the volume was made up to 2 mL.

Table 1
Crystal data and structure refinement for compounds **1** and **2**.

Compound	**1**	**2**
CCDC No.	903577	903578
Empirical formula	$C_9H_{11}N_3O$	$C_{14}H_{14}ClN_5OPd$
Formula weight	177.21	410.15
T (K)	298(2)	298(2)
Wavelength (Å)	0.71073	0.71073
Crystal system	monoclinic	tetragonal
Space group	$P2_1$	$I4_1/a$
Unit cell dimensions		
a (Å)	6.9503(5)	22.5744(3)
b (Å)	6.4535(3)	22.5744(3)
c (Å)	10.1631(6)	13.2967(2)
β [°]	93.418(4)	90
V (Å^3)	455.04(5)	6776.05(16)
Z	2	16
ρ_{Calcd} (g/cm^3)	1.293	1.608
Absorption coefficient (mm^{-1})	0.089	1.260
F(000)	188	3264
Crystal size (mm)	0.12 × 0.04 × 0.06	0.20 × 0.20 × 0.15
θ (°)	2.01–25.50	1.78–25.04
Limiting indices	$-8 < h < 8$, $-7 < k < 7$, $-11 < l < 12$	$-26 < h < 24$, $-22 < k < 26$, $-15 < l < 15$
Reflections collected/ unique (R_{int})	6566/1712 (0.0301)	25760/3001 (0.0335)
Completeness to theta = 25.50 (%)	100.0	100
Data/restraints/parameters	1712/1/119	3001/0/199
R_1, all data, R_1 [$I > 2\sigma(I)$]	0.0499, 0.0560	0.0254, 0.0343
wR_2, all data, wR_2 [$I > 2\sigma(I)$]	0.1382, 0.1452	0.0677, 0.0726
Goodness-of-fit (GOF) on F^2	1.049	1.064
Largest difference in peak and hole (e Å^{-3})	0.243 and −0.195	0.366 and −0.212

Table 2
Selected bond distances (Å) and angles (°) for **1** and **2**.

*Compound **1***			
C1–C7	1.499(3)	C7–C8	1.464(3)
C8–C9	1.498(3)	N2–N3	1.363(3)
N1–O1	1.403(3)	C7–N2	1.293(3)
C2–C1–C7	120.8(2)	N1–C8–C7	113.5(2)
C7–N2–N3	117.6(2)	C8–N1–O1	114.1(2)
*Compound **2***			
Pd1–N1	1.984(2)	C1–C7	1.499(4)
Pd1–N2	2.001(2)	C2–C3	1.377(4)
Pd1–N4	2.016(2)	C3–C4	1.363(5)
Pd1–Cl1	2.3109(8)	C4–C5	1.372(5)
N1–O1	1.275(3)	C5–C6	1.373(5)
N1–C8	1.327(4)	C7–C8	1.426(4)
N2–C7	1.321(4)	C8–C9	1.494(4)
N2–N3	1.372(3)	C10–C11	1.440(4)
N3–C10	1.283(4)	C11–C13	1.370(4)
N4–C12	1.311(4)	C12–N5	1.332(4)
N4–C11	1.379(4)	C13–C14	1.493(4)
C1–C2	1.381(4)	C1–C6	1.379(4)
N1–Pd1–N2	80.28(9)	C10–N3–N2	117.8(2)
N1–Pd1–N4	171.42(10)	C12–N4–C11	106.2(2)
N2–Pd1–N4	91.91(9)	C12–N4–Pd1	132.2(2)
N1–Pd1–Cl1	95.61(7)	C11–N4–Pd1	120.90(19)
N2–Pd1–Cl1	172.84(7)	N2–C7–C8	116.6(3)
N4–Pd1–Cl1	92.51(7)	N2–C7–C1	122.7(3)
O1–N1–C8	119.7(2)	C8–C7–C1	120.7(3)
O1–N1–Pd1	125.43(19)	N1–C8–C7	114.4(3)
C8–N1–Pd1	114.8(2)	N1–C8–C9	119.6(3)
C7–N2–N3	116.1(2)	C7–C8–C9	125.8(3)
C7–N2–Pd1	112.97(19)	N3–C10–C11	133.1(3)
N3–N2–Pd1	130.53(18)		

2.3.3. Determination of MIC

The determination of the MIC was done by the agar disk diffusion method [26] and confirmed by an INT assay. For disk diffusion,

Table 3
Hydrogen bonds (Å and °) for **1** and **2**.

D–H···A	*d*(D–H)	*d*(H···A)	*d*(D···A)	∠(D–H–A)	Symmetry code
Compound ***1***					
O1–H1···N2	0.82	2.17	2.894(3)	147.8	$x, y+1, z$
N3–H3B···N1	0.86	2.28	2.937(3)	133.6	$x, y-1, z$
Compound ***2***					
N5–H5A···Cl1	0.86	2.80	3.385(3)	126.8	$y-1/4, -x+5/4, -z+5/4$
N5–H5A···O1	0.86	2.01	2.755(3)	144.4	$y-1/4, -x+5/4, -z+5/4$

a 0.1 mL standard suspension of bacteria (2 x 10^6 CFU/mL) was spread over Muller-Hinton agar plates and disks containing drugs of different concentrations were placed on every type of microorganism containing plate. The inoculated plates were incubated at 37 °C for 24 h and observed for a zone of inhibition. The obtained MIC values were confirmed by an INT assay where two sets of nutrient broth were prepared to which 0.1 mL standard suspension of bacteria (2 x 10^6 CFU/mL) were added. To one set, a specific amount of drug (10, 25, 50, 100, 200 and 400 μg/mL) was added, and another set was taken as a control, then finally *p*-iodo-nitrotetrazolium chloride (INT assay) was added and incubated at 37 °C for 24 h.

3. Results and discussion

3.1. Synthesis and formulation

The ligand employed for the present work is 1-(4-methylimidazol-5-yl) phenylhydrazonopropane-2-one oxime (LH), a Schiff-base ligand. LH has been synthesized by the Schiff-base condensation of equimolar proportions of 1-hydrazono-1-phenyl-propan-2-one oxime (**1**) and 4-methylimidazole-5-carboxaldehyde in methanol. The reaction of LH with $Na_2[PdCl_4]$ in a 1:1 M proportion in methanol gives rise to the brown monomeric Pd(II) compound, [Pd(L)(Cl)] (**2**). The formation of the compound was established from the presence of a positive FAB-MS peak in *m*-nitrobenzyl alcohol (MNBA) matrix at 374.1 (Calc. 374.5; 100% intensity) corresponding to $[Pd(L)]^+$ for **2**. The C, H and N microanalytical data of the single crystals of **2** also corroborate the above formulation. The compound is diamagnetic, suggesting a square-planar disposition of the palladium center in **2**. The synthetic scheme is outlined below (see Scheme 1):

The diamagnetic nature of **2** enables us to detect all the carbon nuclei in its 500 MHz ^{13}C NMR spectrum in DMSO-d_6 (Fig. 1 as Supplementary Data). The bands associated in the infrared spectrum of free LH with *ν* 1616(s) [*ν*(C=N)], 1462(s) [*ν*(C=N of oxime)] and 1188(s) cm^{-1} [*ν*(N–O)] appear respectively at wavenumbers 1609, 1451 and 1206 cm^{-1} in **2**. The *ν*(Pd–Cl) vibrational modes, which typically range between 300 and 400 cm^{-1} [27] could not be observed within the window of the spectrometer used (4000–400 cm^{-1}) here. However, the *ν*(Pd–N) mode is discerned at 441 cm^{-1} [28].

The electronic spectra of Pd(II) complexes are indicative of their square-planar geometries. In the electronic spectrum of **2** in DMF, only one d–d band at 502 nm was observed, which is assigned to the d_z^2 to $d_{x^2-y^2}$ transition [18]. This is indicative of a low-spin complex of a d^8 metal ion with a square-planar geometry. The molar electrical conductivities of $\sim 10^{-3}$ M solutions of complex **2** in DMF (58 Ω^{-1} cm^2 mol^{-1}) and DMSO (11 Ω^{-1} cm^2 mol^{-1}) indicate the non-electrolytic nature of **2** in both the solvents [29].

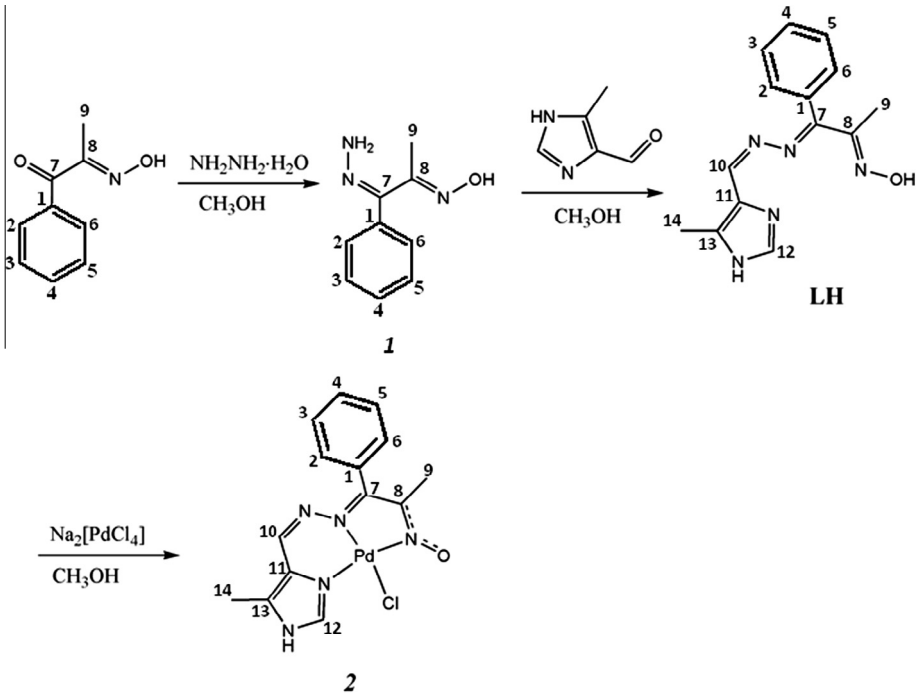

Scheme 1. Ligand and compound structures along with the atom numbering for NMR spectroscopic assignments.

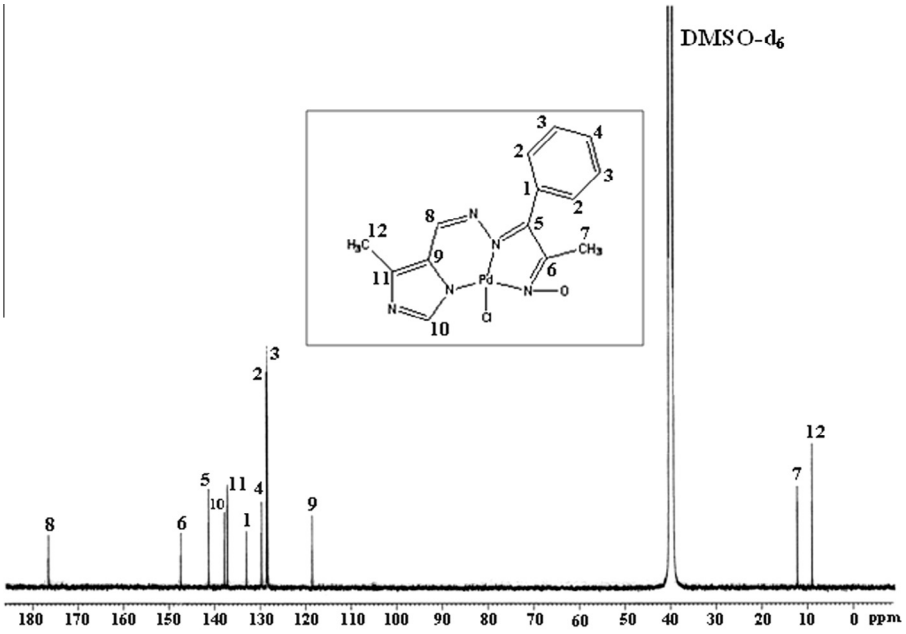

Fig. 1. ^{13}C NMR spectrum of [Pd(L)Cl] (**2**) in DMSO-d_6.

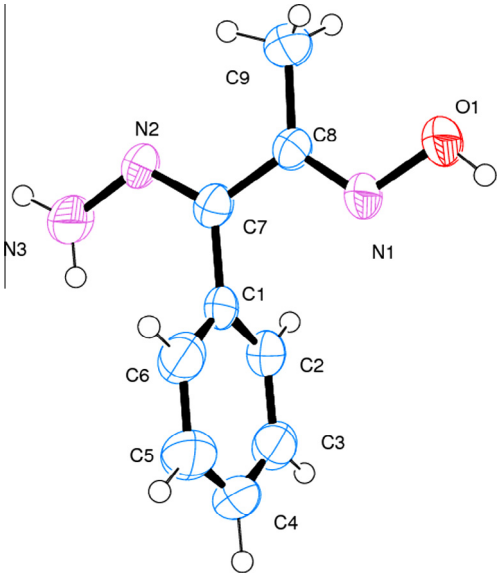

Fig. 2. The structure of **1** with ellipsoids at 50% probability.

3.2. Molecular structures

3.2.1. 1-hydrazono-1-phenyl-propan-2-one oxime (*1*)

The solid state structure of **1** was established through X-ray crystallography. The molecular structure and the atom numbering scheme for **1** is shown in Fig. 2. A packing diagram of the hydrogen bonded polymeric network is shown in Fig. 3. Selected metrical parameters for this structure are summarized in Table 2. The compound crystallizes in the monoclinic space group $P2_1$ with two molecular weight units accommodated per unit cell. The N2–N3 bond distance is 1.363(3) Å. The trans angles C9–C8–C7 and C1–C7–C8 are 121.1(2)° and 118.82(19)° respectively. The C8–N1 and N1–O1 bond distances of the oxime function in **1** respectively have values of 1.276(3) and 1.403(3) Å. Similar magnitudes of the C–N and N–O bond distances, 1.290(6) and 1.397(5) Å respectively, for an oxime moiety can be found in 1-phenyl-1-{N(4)-methylthiosemicarbazone}-2-oximepropane (H_2Po4M) [30]. The crystal structure of H_2Po4M was found to have the oxime and thiosemicarbazone moieties on opposite sides of the carbon–carbon backbone. The relative dispositions of the functionalities as found in H_2Po4 M is akin to our case. In **1**, the oxime and the hydrazone moieties are on the opposite sides of the C7–C8 bond. The C8–N1–O1 angle of the oxime function is 114.1(2)°. The magnitude of the torsion angle around C7–C8 seems to be very informative. A close value of the torsion angle, C–C=N–O to 0° corresponds to the *cis* configuration; while it is 180° for a *trans* configuration of the oxime function with respect to the C–C connectivity. In **1**, the C7–C8–N1–O1 torsion angle is 179.32(17)°, as found from X-ray crystallography. Thus the oxime group in **1** adopts a clear *trans*-planar arrangement with respect to the C7-C8 linkage. Again, the torsion angle C8–N1–O1–H1 is 172.49 °. The O-H bond may be *syn-planar* or *anti-periplanar* to C=N. Though the *anti-periplanar* conformation is common, a few cases are also known where the *syn-planar* situation (torsion angle close to 0°) are also known [31]. This difference in conformation arises due to rotation around the C–C single bond, the connector in a heterodiene system. In our case this connector is the C7–C8 bond. This bond length is 1.464(3) Å, a value considerably shorter than the theoretical $C(sp^2)$–$C(sp^2)$ single-bond (1.48 Å). For oximes having co-planar conjugated double bonds, this bond length lies in the range of 1.47–1.50 Å [32]. Thus the shrinkage of the C7–C8 bond length in **1** from the ideal C–C single bond length may be due to the development of a partial double bond character due to delocalization in this heterodiene system.

In a monoxime having two double bonds (inclusive of the oxime moiety), three possible isomers are possible, *syn,syn*, *syn,anti* and *anti,anti* [33]. **1** has two such centers due to the presence of the C8=N1 and C7=N2 double bonds. With respect to these, **1** is the *syn*-methyl and *syn*-phenyl isomer, as found in its solid state structure (Fig. 2).

The O1–H1···$N2^i$ (i $x, y + 1, z$) hydrogen bond in **1** (Fig. 3), with donor O1–H1 (0.82 Å) and acceptor H1···$N2^i$ (2.17 Å), has been detected by X-ray crystallography (Table 3). Though the position of the H atom, as deciphered from X-ray crystallography, has been

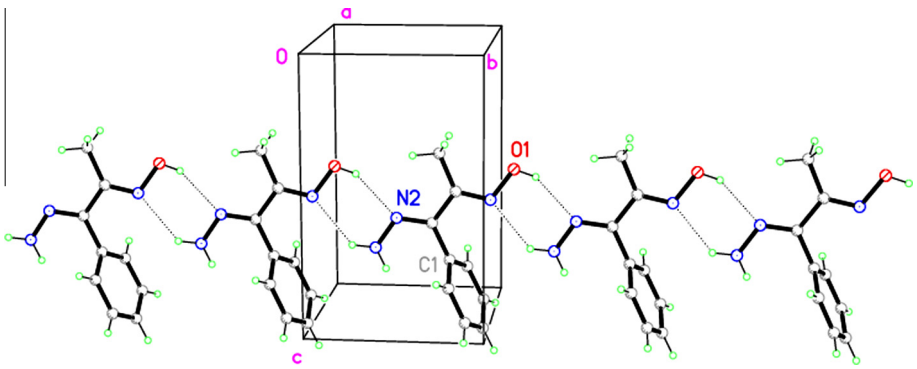

Fig. 3. The packing diagram of **1** showing the H-bonding motifs: R_2^2 (6) and C_1^1 (6).

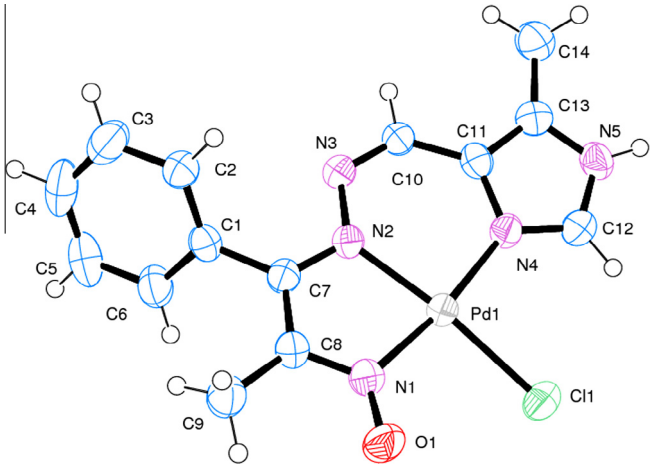

Fig. 4. The structure of [Pd(L)(Cl)] (**2**) with ellipsoids at 50% probability.

calculated (riding model), it seems that the H atom of the O1–H1···N2 hydrogen bond in **1** is closer to the O1 center by a value of 0.7 Å from the baricentre of the O1–N2 bond (2.894 Å). There are only a few examples of X-ray crystal structures with O–H···N bonds in which the H atom has at least similar distances to O and N, with O–H and H···N distances of 1.23 and 1.29 Å respectively [34,35]. However the first O–H···N hydrogen bond with a centered proton, as detected by Neutron Diffraction (ND) at 20 K, has an O···N distance of 2.506 Å [36]. To date, this is the shortest known O–H···N hydrogen bond for which ND data is available. In our case this O–H···N distance is 2.894 Å, a value significantly larger than 2.506 Å. Thus based on this distance criterion alone, the O1–H1···N2 hydrogen bond in **1** is weak indeed. In light of the similar distance criterion, N3–H3B···N1^{ii} (ii x, $y-1$, z) is also weak.

3.2.2. [Pd(L)(Cl)] (**2**)

The solid state structure of **2** was determined through X-ray crystallography. The molecular structure and the atom labeling scheme for **2** is shown in Fig. 4. A packing diagram along with the H-bonded network of **2** is shown in Fig. 5. Selected metrical parameters for the structure of **2** are also summarized in Table 2. The compound crystallizes in the tetragonal space group $I4_1/a$, with sixteen molecules in the unit cell. The palladium center in **2** is nested in an 'N$_3$Cl' core. The Pd1–N1, Pd1–N2 and Pd1–N4 bond distances are 1.984(2), 2.001(2) and 2.016(2) Å respectively. A monomeric palladium(II) complex having an 'N$_3$Cl' coordination

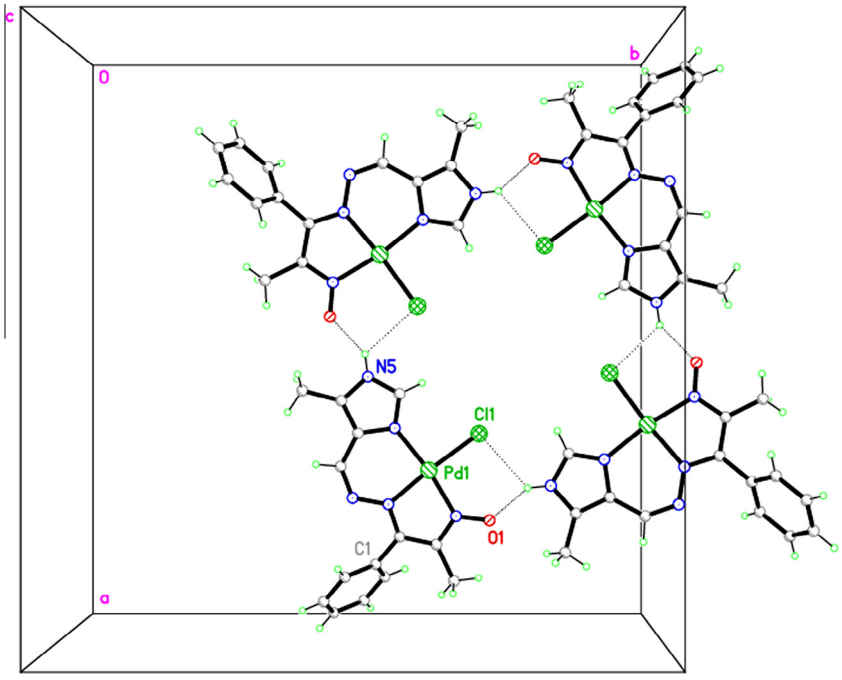

Fig. 5. H-bonding motif: R_4^4 (28) in **2**.

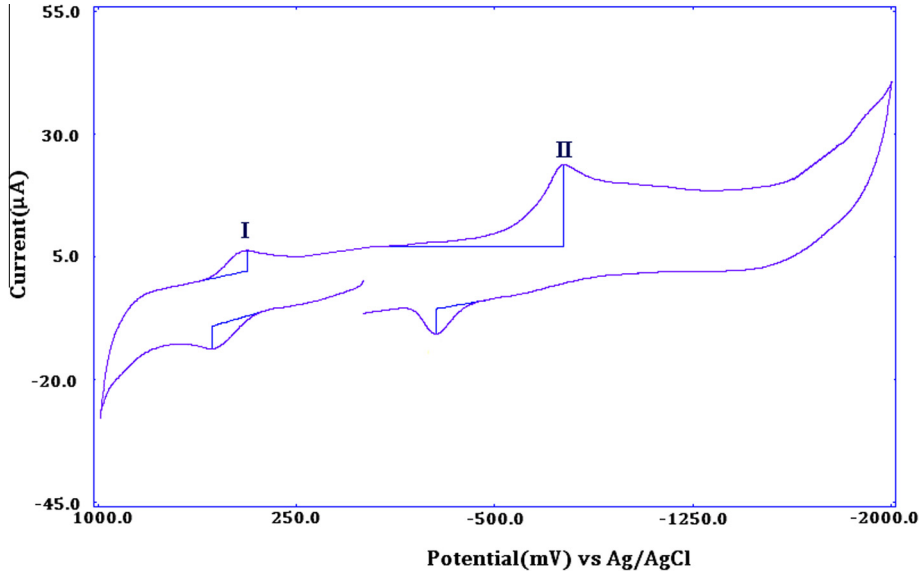

Fig. 6. CV of **2** in DMF at a scan rate of 200 mV s^{-1}. The analyte concentration was 6.095×10^{-4} (M).

environment for Pd is known [37], with which we can compare our Pd–N bond lengths. Here the three Pd–N bond distances are 1.9796, 2.0117 and 2.1065 Å, and these values are comparable to **2**. Again, all these values match well with the literature value (2.02 to 2.04 Å) [38].

The *cis*-(N1–Pd1–N2, N2–Pd1–N4, N1–Pd1–Cl1, N4–Pd1–Cl1) and the *trans*-(N1–Pd1–N4, N2–Pd1–Cl1) angles lie respectively in the ranges 80.28–95.61 and 171.42–172.84°, deviating copiously from 90° and 180°. Thus the geometry around the palladium(II) center in **2** is quite distorted. The palladium center is displaced by 0.029(1) Å from the mean square-plane defined by N1, N2, N4 and Cl1. The core is nevertheless essentially planar. Additionally, in order to estimate the geometric shape of **2**, the Addison angular structural parameter (τ) has been calculated [39,40]. For four coordinated complexes, this parameter τ_4 is defined as $\tau_4 = [360-(\alpha + \beta)]/141$ where α is the largest angle and β is the second largest angle around the central metal atom in question. A value of 0 for τ_4 is the signature for a perfect square-planar geometry, while it is unity for a regular tetrahedral core [40]. Taking N2-Pd1-Cl1 = 172.84° (α) and N1-Pd1-N4 (β) = 171.42°, the τ_4 value comes out as 0.112 for **2**. This value is close to 0. Thus the geometry around the palladium center is square-planar. However, it is slightly distorted. The sum of the angles around the palladium is 360.31°, a value quite close to 360°. This is due to the chelate effects around the Pd ion, with 5- and 6-membered planar rings, which bring about stability to the structure. The packing diagram of **2** shows the intermolecular hydrogen bonding. This H-bonding consists exclusively of classical N–H···O bonds.

3.3. Electrochemistry

The redox behavior of the title compound **2** has been studied by cyclic voltammetry in DMF at a GC working electrode under N_2 atmosphere. The resulting cyclic voltammogram (CV) is shown in Fig. 6 and the peak potentials are tabulated in Table 4. On the positive side of the Ag/AgCl reference electrode, **2** exhibits one anodic wave (Couple-I) with a peak potential of 0.573 V versus Ag–AgCl. The associated peak current, i_{pa}, is 4.49 μA. The corresponding cathodic response is discernable in the subsequent reverse cycle with a peak potential value of 0.443 V versus Ag–AgCl, having a peak current, i_{pc}, of 4.21 μA. Thus this oxidation can safely be assigned as metal centered. A comparison of the voltammetric peak currents with those of the ferrocene-ferrocenium couple (0.44 V versus Ag/AgCl) under the same experimental conditions establishes that the present oxidative response in **2** involves one electron. So, $E_{½}$ at + 0.508 V versus Ag–AgCl corresponds to a Pd(II) to Pd(III) oxidation. The ratio of i_{pc} to i_{pa} is 0.937, a value close to unity. Thus this oxidative response is quasi-reversible in nature. This observed value of the Pd(III)/Pd(II) redox couple is comparable with the value reported earlier [41,42].

Our palladium(II) complex again shows only one electrochemical response at a $E_{½}$ value of -0.516 V (Couple II) on the negative side of the Ag/AgCl reference electrode. Again, comparison of the voltammetric peak currents of couple II with those of the ferrocene-ferrocenium couple (0.44 V versus Ag/AgCl) under the same experimental conditions establishes that the present reductive responses in **2** involve one electron only. Thus the above reductive response can be assigned as Pd(II) to Pd(I). The cathodic peak potential and peak current of couple II are −0.757 V and 16.67 μA, respectively. The subsequent anodic response in the reverse cycle can be discernable at −0.274 V versus Ag–AgCl with an anodic peak current, i_{pa}, of only 5.04 μA. The ratio of i_{pc} to i_{pa} is 3.307. This value shows a considerable deviation from unity. The cathodic peak current, i_{pc}, increases with the square root of the scan rate ($v^{1/2}$), but not in proportionality. Again, the cathodic peak potential, E_{pc}, shifts more negatively with the increase in sweep rate, ν. Judged on these criteria, the metal centered reduction for **2** at peak II is said to be quasi-reversible in nature [43]. Those CV effects might be due to involvement of ligand orbital electrons as well. However the ligand LH does not show any voltammogram in the potential range of interest here under identical conditions, namely solvent, three-electrode assembly, supporting electrolyte, scan rate etc., in which the title palladium(II) compound displays voltammograms. Thus the following plausible metal-centered redox steps might be operative here:

Table 4
Cyclic voltammetric data for **2**.

Entry	E_{pc} (V)	E_{pa} (V)	ΔE (V)	$E^{\circ}_{½}$	i_{pc} (μA)	i_{pa} (μA)
Couple I	0.443	0.573	0.13	0.508	4.21	4.49
Couple II	−0.757	−0.274	0.483	−0.516	16.67	5.04

E_{pc} is the peak potential for the cathodic wave, E_{pa} is the peak potential for the anodic wave, $E_{½} = 0.5\ (E_{pc} + E_{pa})$, i_{pc} is the peak current for the cathodic wave, i_{pa} is the peak current for the anodic wave.

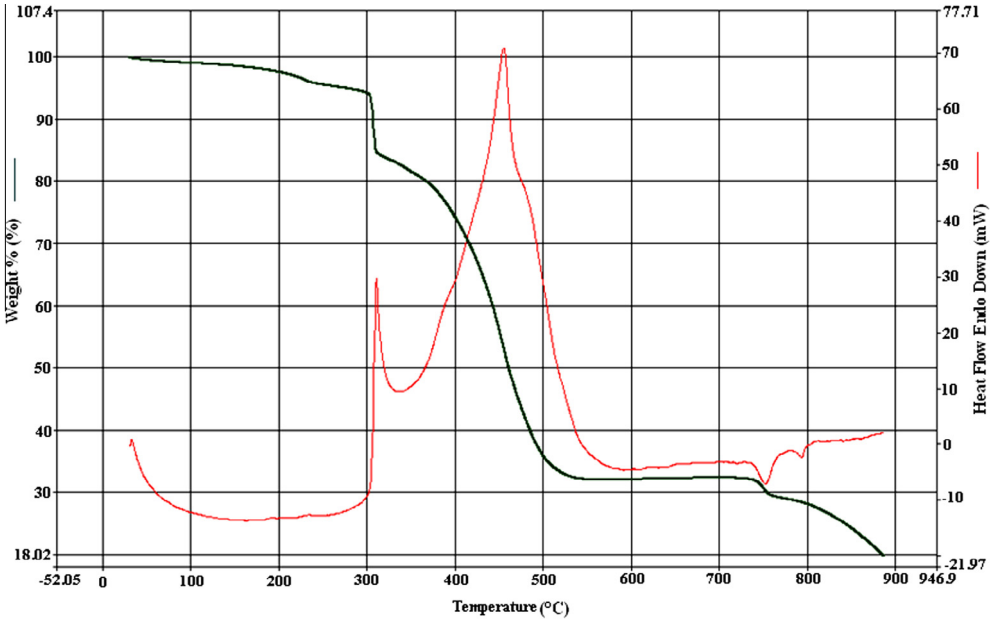

Fig. 7. TG/DTA of [Pd(L)Cl] (**2**).

Couple I: $[Pd^{III}(L)(Cl)]^{+} + e^{-} \rightarrow [Pd^{II}(L)(Cl)]^{0}$ $E_{½} = 0.508$ V
Couple II: $[Pd^{II}(L)(Cl)]^{0} + e^{-} \rightarrow [Pd^{I}(L)(Cl)]^{-}$ $E_{½} = -0.516$ V

3.4. BVS analysis

With a view to assigning the oxidation state of the central palladium center in our complex **2**, we have taken the initiative to perform calculations based on the Bond Valence Sum (BVS) method [44,45]. BVS relates the bond lengths around a metal center to its oxidation state. Developed historically from the concept of bond number, this method was originally propounded by Pauling [46]. Later I. D. Brown and co-workers further fleshed it out [46]. The advantage of this approach is that the bond length is a unique function of bond valence. Generally for a particular bond type, the bond valence diminishes exponentially as the bond length increases In this semi-empirical method, the valence s of a bond between two given atoms *i* and *j* is related by an empirical relation (1)

$$S_{ij} = \exp[(r_o - r_{ij})/0.37] \quad (1)$$

Table 5
Representation of MIC values of drug **2** on the tested organisms.

Organisms	MIC (μg/mL) values of the drug						
	400	200	100	50	25	10	AM
E.coli ATCC 25938	+	+	+	+	+	+	10
S. typhi 62	+	+	+	+	+	+	25
Pseudomonas AMRI 100	+	+	+	+	+	+	100
V. cholerae 20	–	–	–	–	–	+	25
K. pneumoniae 714	+	+	+	+	+	+	100
S. dysenteriae 1	+	+	+	+	+	+	1
S. aureus 29737	+	+	+	+	+	+	5
B. cereus 11778	–	+	+	+	+	+	25
P. aeruginosa 25619	–	–	+	+	+	+	100
B. subtilis 6633	–	–	+	+	+	+	25
B. pumilus 14884	–	–	+	+	+	+	50
B.bronchiseptica 4617	–	–	+	+	+	+	50
S. epidermidis 12228	–	–	–	+	+	+	5
K.pneumoniae 10031	+	+	+	+	+	+	100
M. luteus 10240	–	–	–	+	+	+	5
S. sonnei NK 4010	+	+	+	+	+	+	50
S. typhimurium NTCC 74	+	+	+	+	+	+	25

"+" represents no antimicrobial activity and "–" shows antimicrobial activity (AM – amoxycillin).

where r_{ij} is the length of the bond in Å and r_o is a parameter characteristic of the bond. With the same unit in Å, like r_{ij}, r_0 is known as the bond valence parameter. This parameter is geometry and coordination number specific. The oxidation number N_i of the atom *i* is simply the algebraic sum of these s values of all the bonds (*n*) around the atom I, following equation (2)

$$N_i = \sum_{i=1}^{n} S_{ij} \quad (2)$$

This N_i is known as the BVS of the ith atom. Thus if r_0 is known for a particular bond type, the BVS can be calculated from the crystallographically determined r_{ij} values. Taking r_0 values for Pd–N and Pd–Cl bonds of 1.81 and 2.05 Å respectively [47], the BVS for the palladium center in **2** comes out as 2.288 valence units (vu). This value closely approaches the error limit of ±0.250 vu as proposed earlier by Thorp [48,49]. Thus an oxidation number of +2 can safely be assigned to the palladium center in **2** computationally.

3.5. Thermal behavior

The thermal behavior (TGA and DTA) of **2** have been studied (Fig. 7) within the temperature range 30.0–900.0 °C in a dynamic N_2 atmosphere (flow rate = 20.0 mL/min). 3.970 mg of **2** was heated in a platinum crucible at a heating-rate of 15.0 °C per minute. Dried and purified α-Al_2O_3 powder was used as a reference in our case. Thermogravimetric (TG) analysis confirms that **2** is thermally stable up to ca. 300 °C. The thermogram shows sequential events of weight loss. Within the temperature range 300–312.5 °C, the experimental mass loss of 9.4% is in fair conformity with the theoretical loss (8.7%) for the complete removal of the bonded chloride atom per formula unit. The corresponding differential thermal analysis (DTA) curve shows one exothermic peak at ca. 315 °C. The second weight loss is associated within the temperature range 313–534 °C. This is due to ligand combustion. The experimental weight loss was 52.3% against the calculated loss of 56.8%. This combustion is accompanied by a large exothermic heat loss. The respective DTA peak is found at 450 °C. Up to 900 °C, the mass loss is virtually complete. The final decomposition product is

Table 6
Representation of the zone diameter of the MIC values of drug **2** on tested organisms.

Organisms	Zone diameter of MIC (mm)
V. cholerae 20	10 ± 0.1
B. cereus 11778	15 ± 0.2
P. aeruginosa 25619	14 ± 0.2
B. subtilis 6633	10 ± 0.2
B. pumilus 14884	10 ± 0.2
B. bronchiseptica 4617	13 ± 0.2
S. epidermidis 12228	10 ± 0.1
M. luteus 10240	15 ± 0.2

elemental palladium, as indicated by the weight of 11.8% (Theo. 12.6%). It is pertinent to note that for palladium complexes, the final residue in the thermal analysis is metallic palladium [50,51].

3.6. Antimicrobial activity

Our compound **2** shows antimicrobial properties. However, the ligand, LH does not. The drug **2** was effective against 8 tested organisms among the listed organisms in Table 5.

The lowest MIC value of **2** was found at a concentration of 25 μg/mL and the highest concentration was 400 μg/mL. The drug's inhibitory effect was against *V. cholerae* VC 20 at a concentration 25 μg/mL and *Micrococcus luteus* 10240 and *Streptococcus epidermidis* 12228 at 100 μg/mL.

From the results against the microorganisms of the test samples we can conclude that **2** shows a broad spectrum, i.e. effective on both Gram positive and Gram negative organisms. **2** is more effective on enteric organisms.

The zone of inhibition of the test samples was evaluated by the well diffusion method [24]. 0.1 mL of bacterial solution (2×10^6 CFU/mL) was transferred to Mueller–Hinton agar plates. The bacterial suspensions were uniformly spread over a number of plates using a sterile glass spreader. For each type of organisms a particular concentration of drug solution was impregnated into the agar plates of the screened 8 microorganisms (Table 6). All the agar plates were then incubated at 37 °C for 24 h. The sensitivity was evaluated by measuring the presence of a clear zone of inhibition on the agar surface around the wells.

The killing rate of the tested compounds was determined by using viable cell count experiments [52]. The microbial suspension was diluted with sterile distilled water up to 2×10^6 CFU/mL. Two sets of test were taken as a control. Both sets of test tubes were incubated at 37 °C and at regular intervals of 0, 2, 4, 6 and 18 h, a 0.1 mL sample was withdrawn and diluted 100 times in a sterile test tube with sterile distilled water and spread over sterile tubes containing Muller-Hinton broth. In one set of test tubes, 1 mL of bacterial suspension and the drug sample in the MIC range were added and the another set contained a bacterial suspension without the drug sample agar plates. Then the spread plates were incubated overnight at 37 °C. After incubation the colonies were counted in the plates and the reduction in colonies of the test samples were calculated by comparing to the colonies in the control plates.

The results for each type of the 8 microorganisms screened previously have been shown graphically with the respective numerical logarithmic values of the number of colonies after incubation in Figs. 8–15 (Supplementary data). Pertinent data are summarized in Table 7 (Supplementary data).

By analyzing the bacterial growth curves, we can conclude that our Pd(II) compound (**2**) inhibits growth of the tested bacterial strains at the MIC and exerts its effect as a bacteriostatic agent. The probable mechanism of action of **2** against the above microorganisms can only be deciphered by further studies.

4. Conclusions

Here we have synthesized and structurally characterized a neutral and diamagnetic Pd(II) compound (**2**) from an oxime-based ligand, 1-(4-methylimidazol-5-yl) phenyl-hydrazonopropane-2-one oxime (LH). The X-ray crystal structures of both 1-hydrazono-1-phenyl-propan-2-one oxime (**1**) and **2** have been determined. The palladium center is in a square-planar 'N_3Cl' coordination sphere. The BVS method of calculations were also undertaken to assign the oxidation state of palladium and to substantiate the stability of **2**. Electrochemical studies in DMF show a Pd(II) to Pd(III) oxidation at 0.573 V, along with a reduction of Pd(II) to Pd(I) at −0.757 V versus Ag/AgCl. Compound **2** shows antimicrobial activity against a good number of both Gram positive and Gram negative bacteria. Thus our title compound **2** may be developed as a new antimicrobial agent.

Acknowledgements

J.P.N. gratefully acknowledges the University Grants Commission (UGC), New Delhi, India for financial support [F. No. 41-220/2012 (SR)]. M.L.Z and L.P.L. appreciated the NSFC (Grant Nos. 21171109 and 21271121), SRFDP (Grant Nos. 20111401110002 and 20121401110005), the Natural Science Foundation of Shanxi Province of China (Grant Nos. 2010011011-2 and 2011011009-1) and the Shanxi Scholarship Council of China (2012-004). We solicit to bestow our gratitude to the reviewers for helping us in the course of a revision of this paper.

Appendix A. Supplementary data

CCDC 903577 and 903578 contains the supplementary crystallographic data for **1** and **2**. These data can be obtained free of charge via http://www.ccdc.cam.ac.uk/conts/retrieving.html, or from the Cambridge Crystallographic Data Centre, 12 Union Road, Cambridge CB2 1EZ, UK; fax: (+44) 1223 336 033; or e-mail: deposit@ccdc.cam.ac.uk. Supplementary data associated with this article can be found, in the online version, at http://dx.doi.org/10.1016/j.poly.2013.03.064.

References

[1] J. Traeger, T. Klamroth, A. Kelling, S. Lubahn, E. Cleve, W. Mickler, M. Heydenreich, H. Müller, H. Holdt, Eur. J. Inorg. Chem. (2012) 2341.
[2] J. Tsuji, Synthesis with Palladium Compounds, Springer, Berlin, Heidelberg, New York, 1980.
[3] P.M. Maitlis, The Organic Chemistry of Palladium, Academic Press, New York, 1971.
[4] M.J. Cleare, Coord. Chem. Rev. 12 (1974) 349.
[5] N. Miyaura, A. Suzuki, Chem. Rev. 95 (1995) 2457.
[6] A.F. Littke, G.C. Fu, Angew. Chem., Int. Ed. 41 (2002) 4176.
[7] W. Zhang, M. Shi, Tetrahedron Lett. 45 (2004) 8921.
[8] F. Alonso, I.P. Beletskaya, M. Yus, Tetrahedron 64 (2008) 3047.
[9] R.F. Heck, Acc. Chem. Res. 12 (1979) 146.
[10] A.B. Dounay, L.E. Overman, Chem. Rev. 103 (2003) 2945.
[11] K.M. Dawood, Tetrahedron 63 (2007) 9642.
[12] K.M. Dawood, A. Kirschning, Tetrahedron 61 (2005) 12121.
[13] H. Daghriri, F. Huq, P. Beale, Chem. Rev. 248 (2004) 119.
[14] E. Gao, L. Lin, L. Liu, M. Zhu, B. Wang, X. Gao, Dalton Trans. 41 (2012) 11187.
[15] A.S. Abu-Surrah, M. Kettunen, Curr. Med. Chem. 13 (2006) 1337.
[16] A.I. Matesanz, C. Hernandez, A. Rodriguez, P. Souza, J. Inorg. Biochem. 105 (2011) 1613.
[17] A. Garoufis, S.K. Hadjikakou, N. Hadjiliadis, Coord. Chem. Rev. 253 (2009) 1384.
[18] M.N. Patel, P.A. Dosi, B.S. Bhatt, Inorg. Chem. Commun. 21 (2012) 61.
[19] Bruker, SMART (Version 5.0) and SAINT (Version 6.02), Bruker AXS Inc., Madison, Wisconsin, USA, 2000. .
[20] G.M. Sheldrick, Acta Crystallogr., Sect. A 64 (2008) 112.
[21] A.L. Spek, J. Appl. Crystallogr. 36 (2003) 7.
[22] K.B. Sahu, S. Ghosh, M. Banerjee, A. Maity, S. Mondal, R. Paira, P. Saha, S. Naskar, A. Hazra, S. Banerjee, A. Samanta, N.B. Mondal, Med. Chem. Res. 22 (2013) 94.

[23] M.K. Paira, T.K. Mondal, D. Ojha, A.M.Z. Slawin, E.R.T. Tiekink, A. Samanta, C. Sinha, Inorg. Chim. Acta 370 (2011) 175.
[24] National Committee for Clinical Laboratory Standards (NCCLS), approved standard M7–A3, 3rd edn. NCCLS, Villanova, 1993.
[25] J. McFarland, J. Am. Med. Assoc. 14 (1907) 1176.
[26] B. Chakraborty, M.S. Chhetri, S. Kafley, A. Samanta, Indian J. Chem. B49 (2010) (2010) 209.
[27] M. Espinal, J. Pons, J. García-antón, X. Solans, M. Font-bardia, J. Ros, Inorg. Chem. Commun. 12 (2009) 368.
[28] A. Castiñeiras, N. Fernández-Hermida, I. García-Santos, L. Gómez-Rodríguez, Dalton Trans. 41 (2012) 13486.
[29] W.J. Geary, Coord. Chem. Rev. 7 (1971) 81.
[30] W. Kaminsky, J.P. Jasinski, R. Woudenberg, K.I. Goldberg, D.X. West, J. Mol. Struct. 608 (2002) 135.
[31] L. Chertanova, C. Pascard, A. Sheremetev, Acta Crystallogr., B 50 (1994) 708.
[32] H. Saarinen, J. Korvenranta, E. Näsäkkälä, Cryst. Struct. Commun. 6 (1977) 557.
[33] V. Bertolasi, G. Gilli, Acta Crystallogr., B 38 (1982) 502.
[34] F. Takusagawa, K. Hirotsu, A. Shimada, Bull. Chem. Soc. Jpn. 46 (1973) 2292.
[35] Z. Malarski, I. Majerz, T. Lis, J. Mol. Struct. 380 (1996) 249.
[36] T. Steiner, I. Majerz, C.C. Wilson, Angew. Chem., Int. Ed. 40 (2001) 2651.
[37] J.L. Pratihar, P. Pattanayak, D. Patra, C. Lin, S. Chattopadhyay, Polyhedron 33 (2012) 67.
[38] C. Alvariño, A. Terenzi, V. Blanco, M.D. García, C. Peinador, J.M. Quintela, Dalton Trans. 42 (2012) (1998) 11992.
[39] A.W. Addison, T.N. Rao, J. Reedijk, J. van Rijn, G.C. Verschoor, J. Chem. Soc., Dalton Trans. 7 (1984) 1349.
[40] L. Yang, D.R. Powell, R.P. Houser, Dalton Trans. 9 (2007) 955.
[41] Y.Z. Qin, W. Ji, F. Xiao, X. Zhang, S. Jing, Inorg. Chem. Commun. 20 (2012) 177.
[42] D.K. Demertzi, A. Domopoulou, M.A. Demertzis, A. Papageorgioub, D.X. West, Polyhedron 16 (1997) 3625.
[43] R. Greef, R. Peat, L.M. Peter, D. Pletcher, J. Robinson, Instrumental Methods in Electrochemistry, Ellis Horwood Limited, England, 1985. p. 188.
[44] I.D. Brown, D. Altermatt, Acta Crystallogr., Sect. B 41 (1985) 244.
[45] J.P. Naskar, S. Hati, D. Datta, Acta Crystallogr., Sect. B 53 (1997) 885.
[46] I.D. Brown, Chem. Soc. Rev. 109 (2009) 6858.
[47] N.E. Brese, M. O'Keeffe, Acta Crystallogr., Sect. B 47 (1991) 192.
[48] H.H. Thorp, Inorg. Chem. 31 (1992) 1585.
[49] W. Liu, H.H. Thorp, Inorg. Chem. 32 (1993) 4102.
[50] G. Faraglia, D. Fregona, S. Sitran, L. Giovagnini, C. Marzano, F. Baccichetti, U. Casellato, R. Graziani, J. Inorg. Biochem. 83 (2001) 31.
[51] D. Fregona, L. Giovagnini, L. Ronconi, C. Marzano, A. Trevisan, S. Sitran, B. Biondi, F. Bordin, J. Inorg. Biochem. 93 (2003) 181.
[52] J.W. Rhim, S.I. Hong, C.S. Ha, Food Sci. Technol. 42 (2009) 612.